

1 **Changes of the Commensal Microbiome during Treatment are Associated with Clinical**
2 **Response in Nasopharyngeal Carcinoma Patients**

3

4 Tingting Huang^{a,b,c}, Justine Debelius^a, Alexander Ploner^a, Xiling Xiao^d, Tingting Zhang^{b,c},
5 Kai Hu^{b,c}, Zhe Zhang^d, Rensheng Wang^{b,c,#}, Weimin Ye^{a,#}

6

7 ^aDepartment of Medical Epidemiology and Biostatistics, Karolinska Institutet, Stockholm,
8 Sweden

9 ^bDepartment of Radiation Oncology, The First Affiliated Hospital of Guangxi Medical
10 University, Nanning, P. R. China

11 ^c Radiation Oncology Clinical Medical Research Center of Guangxi, Nanning, Nanning, P. R.
12 China

13 ^dDepartment of Otolaryngology-Head & Neck Surgery, First Affiliated Hospital of Guangxi
14 Medical University, Nanning, P. R. China.

15

16 Running title: Microbiome is Associated with Clinical Response in NPC

17

18 # Address correspondence to Weimin Ye (weimin.ye@ki.se) and Rensheng Wang
19 (wangrenshenggxmu@gmail.com).

20 Weimin Ye and Rensheng Wang contributed equally to this work. Author order was
21 determined by consortium policy.

22 **Abstracts**

23 The human microbiome has been suggested to be involved in the regulation of response to
24 anticancer therapies. However, little is known regarding changes of commensal microbes in
25 cancer patients during radiotherapy and whether these changes are associated with response to
26 treatment. We conducted a prospective, longitudinal cohort with sixty-two newly diagnosed
27 nasopharyngeal carcinoma (NPC) patients who were scheduled for radiotherapy-based
28 treatment. Nasopharyngeal swabs were collected longitudinally before radiotherapy, during
29 radiotherapy, and after radiotherapy. The nasopharyngeal microbiome was assessed using 16S
30 rRNA amplicon sequencing. All patients were followed up to 24 months to define an early or
31 late clinical response. We demonstrated the beta-diversity of the nasopharyngeal microbiome
32 showed temporal changes throughout treatment. The magnitude of changes was stably and
33 significantly different between the early and late responders. The temporal microbial
34 networks among NPC patients with early response differed significantly from those with late
35 response. Seven amplicon sequence variants (ASVs) mapped to *Corynebacterium* were lost
36 during treatment. Twenty-eight abundant ASVs differed by patients' responses throughout
37 treatment. Among them, 10 ASVs differed between the early responders and late responders
38 before getting any treatment and the difference was consistent along the radiotherapy course.
39 This study addressed the temporal changes of the nasopharyngeal microbiome in NPC
40 patients during radiotherapy and suggested a significant association with clinical response.
41 The subject-specific changes of the nasopharyngeal microbiome might serve as a potential
42 predictor for clinical response to radiotherapy.

43

44 **Importance**

45 The human microbiome has been suggested to be involved in the regulation of response to
46 anticancer therapies. However, little is known regarding changes of commensal microbes in
47 cancer patients during radiotherapy and whether these changes have an impact on response to
48 treatment. In this longitudinal study of nasopharyngeal carcinoma patients, we demonstrate
49 that the temporal changes of the nasopharyngeal microbiome in NPC patients during
50 radiotherapy-based treatment and suggest a significant association with patients' clinical
51 response. We identify 28 abundant amplicon sequence variants differed significantly between
52 the early and late responders throughout treatment. Among them, 10 are consistently differed
53 by patients' responses. These subject-specific changes might serve as a potential predictor for
54 clinical response to radiotherapy. To the best of our knowledge, this is the first example that
55 the commensal microbiome may influence the response to radiotherapy-based treatment in
56 cancer patients.

57 **Introduction**

58 The human commensal microbiome has been suggested to be involved in both carcinogenesis
59 and in the regulation of response to anticancer therapies (1-4). Accumulating evidence
60 suggests that the microbiome can substantially affect the effectiveness of chemotherapy and
61 immunotherapy such as gemcitabine and immune checkpoint inhibitors (5, 6). Accordingly,
62 there is a growing interest in identifying and targeting these microbes in the anti-cancer
63 treatment. However, little is known regarding whether or how the microbiome may regulate
64 the response to radiotherapy, which is critical to the realization of its potential (2, 3, 7). In part,
65 this is due to a lack of well designed longitudinal studies looking at the relationship between
66 microbes and response to radiotherapy is seldom studied (2, 3).

67

68 To address this knowledge gap, we conducted a prospective study to characterize the
69 longitudinal patterns of the commensal microbiome among cancer patients during
70 radiotherapy-based anti-cancer treatment and investigated whether the temporal changes of
71 the microbiome might be associated with patients' clinical response. Nasopharyngeal
72 carcinoma (NPC) is a malignant disease and endemic mainly in southern China and Southeast
73 Asia (8). Radiotherapy is the essential mainstay of curative-intent treatment for the non-
74 disseminated disease. Intensity-modulated radiation therapy (IMRT) contributes to the high 5-
75 year survival rate of 68-80%, together with chemotherapy (9, 10). However, both local and
76 distant failure after a first-line therapy remain key challenges which call for identification of
77 novel indicators and modulators of clinical response. Hence, we prospectively collected
78 nasopharyngeal swab samples during radiotherapy from a hospital-based NPC-patient cohort
79 in southern China where NPC incidence rates exceed 10-15 per 100 000 person-years, about
80 twenty times the rate in the western world (8). We hypothesized that the temporal change of

81 nasopharyngeal microbiome during radiotherapy might be associated with NPC patients'
82 clinical responses.

83

84 **Results**

85 A total of 445 nasopharyngeal microbial profiles, corresponding to 39 NPC patients, were
86 analyzed. Thirty-six (92.3%) patients had advanced disease (stage III to IV_B) at diagnosis. All
87 of the NPC patients were treated with radiotherapy, 35 (89.7%) received concurrent
88 chemotherapy including 25 (64.1%) who received induction chemotherapy or adjuvant
89 chemotherapy. Twenty-seven patients (69.2%) with CR at the first clinical check-up were
90 defined as early responders; the remaining 12 NPC patients achieved CR within 24 months of
91 follow-up were defined as late responders (Supplementary Table S1).

92

93 **NPC patients' clinical responses are associated with the temporal changes of between-** 94 **sample diversity of nasopharyngeal microbiome during radiotherapy**

95 The overall pattern of beta-diversity of the nasopharyngeal microbiome was visualized in
96 PCoA projections for both unweighted and weighted UniFrac distance (Supplementary Figure
97 S1). In both PCoA projections, samples of early responders were relatively dissimilar with the
98 samples of late responders along PC2 (explained 5.88% of the variation in the unweighted
99 projection; and 12.93% of the variation in the weighted projection), while similar along PC1
100 (13.23% in the unweighted, and 29.50% in the weighted) and PC3 (3.59% in the unweighted,
101 and 7.84% in the weighted). By performing volatility analysis, the global variation (as an
102 average) along PCs as a measure of longitudinal temporal volatility is presented in Figure 1.
103 We saw a consistent shift along with the PC1 space with sampling time in both unweighted

104 and weighted panels, regardless of clinical response. In PC2 panels, distinct separations
105 between early and late responders were observed throughout treatment, whereas the temporal
106 trajectories were relatively stable in each group. Moreover, in PC3 space, a moderate
107 separation between the trajectories of response groups was found in the unweighted panel
108 while the trajectories in the weighted panel showed fluctuated and gradual directional changes
109 throughout treatment regardless of response status. The changed volatilities found in the last
110 few sampling time-points have a larger standard deviation compared to the previous time-
111 points, which might be partially explained by low sample numbers. Patient compliance with
112 sample collection varied.

113

114 We measured the rate of change in beta-diversity differences over radiotherapy in terms of the
115 weighted UniFrac step length Δ -wUF and tested whether Δ -wUF changed over treatment and
116 in response to the response status of NPC patients. We found statistically significant evidence
117 for subject-specific differences (random effects) in baseline step length (intercept) as well as a
118 change in step length over sampling time (slope, P -value = 0.0005) from linear mixed effect
119 models (Supplementary Table S2). However, the across-subject average step length (fixed
120 effect) appeared stable in Figure 2A, with no evidence for increasing or decreasing dynamic
121 change (P -value = 0.4609). Adding the clinical response status improved the mixed effect
122 model significantly (P -value = 0.0152). The best-fitting model including clinical response
123 status retained stable for average step lengths for both early and late responders, with larger
124 average step lengths for early responders compared to late responders (Figure 2B). Individual
125 trajectories varied considerably between subjects, shown in Figure 2C.

126

127 **NPC patients' clinical responses are associated with the temporal trajectories of the**
128 **abundant microbial features**

129 Seventy-three ASVs were identified as the abundant subset for feature-based analyses. A
130 Procrustean randomization test and Mantel test based on the Bray-Curtis distance indicated a
131 well concordance between the abundant subset and the full dataset (PROTEST: correlation =
132 0.9669, P -value = 0.001, 999 permutations; Mantel test: correlation = 0.9506, P -value = 0.001,
133 999 permutations; Supplementary Figure S2). NMIT evaluates interdependence networks,
134 which summarized the temporal trajectories of the abundant subset over treatment of each
135 NPC patient into a single distance. The NMIT distances differed between clinical response
136 groups. We observed that the interdependence networks among patients with early response
137 statistically significantly differed from those with a late response, and no statistically
138 significance differences found within response groups (PERMANOVA: P -value = 0.014;
139 permdisp: P -value = 0.315; 999 permutations). In Figure 3, the networks of the late
140 responders varied widely, forming a spread ellipsoid-like cluster, compared to the early
141 responders who formed a smaller and more constrained ellipsoid-like cluster. These clusters
142 are dissimilar along PC1 and PC3, but relatively similar along PC2.

143

144 We investigated longitudinal changes in the abundant ASVs across all samples using a
145 modified ANCOM-test. We identified seven abundant ASVs where more than 80% of ASV
146 ratios were temporally correlated (Supplementary Figure S3, panel A), all members of genus
147 *Corynebacterium*. There was a decrease in the relative abundance of all seven ASVs showed
148 during treatment while most other ASVs remained stable over treatment course
149 (Supplementary Table S3; and Figure S3, panel B to E).

150

151 To quantify ASV-based longitudinal differences between early and late responders, we
152 applied SS-ANOVA. We identified 28 out of 73 abundant ASVs as differing significantly
153 between early and late responders over treatment course, listed in Table 1 (P -value < 0.05,
154 1500 permutations). Notable that, among these significant ASVs, 10 differed between the
155 early responders and late responders before getting any treatment, and remained consistently
156 different during radiotherapy. Additionally, there were 9 ASVs that were similar between
157 response groups during the first one-third of treatment and became different until the
158 completion. In contrast, 5 ASVs differed between groups at the beginning and was converged
159 during treatment.

160

161 For better visualization of the temporal trajectories of the difference between the early and
162 late responders, the log₂-fold changes of the 73 abundant ASVs estimated by SS-ANOVA
163 were plotted as a heatmap and clustered into three groups (Cluster A to C) (Figure 4, and
164 Supplementary Table S4). We found 22 ASVs (30.1%) in Cluster A, which were more
165 prevalent among the early responders while 12 of them were significantly different between
166 response groups with an increased relative abundance along with treatment course. Among
167 the significant ASVs, 4 were members of genus *Burkholderia* (gBurkh.39c8, gBurkh.6364,
168 gBurkh.f802, and gBurkh.ee2f), 2 were genus *Acinetobacter* (gAcine.efe8, and gAcine.32b4),
169 and the rest were members of genus *Corynebacterium* (gCoryn.ca4d), *Streptococcus*
170 (gStrep.3ed3), *Brevundimonas* (gBrevu.1285), *Enhydrobacter* (gEnhyd.0ef3), *Candidatus*
171 *Rhodoluna* (gCandi.9a10), and unspecified order Bacillales (oBacil.0094). In Cluster B
172 (n=37), most of the ASVs had relatively small difference between response groups and were
173 found no statistically significant difference across treatment. Four ASVs showing significant
174 difference across treatment (assigned to genus *Corynebacterium* (gCoryn.1650, gCoryn.5ba9),
175 unclassified family Methylobacteriaceae (fMethy.ebba), and unclassified family

176 Bradyrhizobiaceae (fBrady.cbae)). For Cluster C, 14 ASVs were more among the late
177 responders compared to the early responders with dynamic trajectories (increased, decreased,
178 and relatively stable in difference) over treatment. Twelve of them found statistically
179 significant which were the members of genus *Acinetobacter* (gAcine.4f58, gAcine.4c95, and
180 gAcine.dfae), genus *Thermus* (gTherm.b26c, gTherm.94db, and gTherm.087b), genus
181 *Ralstonia* (gRalst.edc7 and gRalst.a529), genus *Corynebacterium* (gCoryn.ff32, gCoryn.0838),
182 genus *Staphylococcus* (gStaph.ab0b), and unspecified family Caulobacteraceae (fCaulo.a200).

183

184 **Discussion**

185 In the present study, we have addressed temporal changes of the commensal microbiome in
186 response to radiotherapy-based anticancer treatment among NPC patients for the first time. To
187 be specific, the temporal changes in between-sample diversity of the nasopharyngeal
188 microbiome and the abundant microbial features are associated with NPC patients' clinical
189 responses. The longitudinal study design provided a comprehensive view of microbial
190 diversity, an effective way for assessing the microbial correlation networks and an
191 opportunity to reveal the degree of change of the abundant features between time points
192 during the observation period (11). Notably, the subject-specific changes showed in our study
193 might suggest a possibility of using the nasopharyngeal microbiome as a predictor for clinical
194 response.

195

196 We observed that the UniFrac distances used for measuring beta-diversity qualitatively
197 (unweighted) and quantitatively (weighted), on average, showed temporal changes throughout
198 treatment (volatilities along PC1 explaining the largest amount of within-subject changes).
199 Previous studies also described the progressive alteration in the oral microbiome during

200 radiotherapy among NPC patients (12), and the change in gut microbiome in patients after
201 pelvic radiotherapy (13). Remarkably, we found distinct and consistent separations in
202 volatility regarding patients' clinical responses along the PC2, which suggests that a global
203 difference between the early and late responders might have existed before treatment and stay
204 relatively stable afterward until the completion of radiotherapy. We further demonstrated that
205 the magnitude of longitudinal global changes of the nasopharyngeal microbiome was
206 significantly different between response groups, namely the average step length of the early
207 responders was statistically, significantly larger than that of the late responders. However, the
208 magnitude of changes appeared constant within each group along with treatment. These
209 findings challenge the Anna Karenina principle, which suggests the positive prognosis is
210 associated with community stability (14). It may implicate bacterial resilience to radiotherapy
211 as a feature of delayed response. It is reasonable to imagine that such a community might be
212 protective in some way against both radiation-induced perturbations on the microbiome as
213 well as the host.

214

215 In the feature-based analysis, we observed similar characteristics in the NMIT analysis: the
216 temporal changes in microbial networks of NPC patients over treatment were statistically
217 significantly different regarding their clinical responses. The difference observed between
218 groups was not due to a large degree of dispersion within groups. By looking at individual
219 abundant ASV, genera known to dominate the human upper aerodigestive tract:
220 *Corynebacterium*, *Staphylococcus*, *Acinetobacter*, and *Streptococcus* (15, 16), were also
221 found dominant in our study. We found a significant and consistent loss of *Corynebacterium*
222 (including 7 distinct ASVs) over treatment. Oral *Corynebacterium* was reported previously to
223 decrease the risk of head and neck cancer, although the study did not include NPC (17).
224 Members of the genera are also normally, temporally stable in Chinese adults (18).

225 Additionally, we observed that 28 out of 73 abundance ASVs were significantly different in
226 abundance between the early and late responders during treatment. Notably, 10 ASVs
227 primarily found in Cluster C differed between groups before the initiation of radiotherapy-
228 based treatment and consistently differed until the completion. These results correspond to the
229 characteristics observed in the diversity-based analyses above. Moreover, genera *Ralstonia*
230 and *Thermus* have been previously identified as reagent contaminants (19). We found
231 consistent signals for 4 ASVs from these genera (Ther-b26c, Ther-087b, Rals-edc7, and Rals-
232 a529) between response groups, despite sample randomization across plates. These organisms
233 were at very low abundance or absent in early responders, but present in late responders. Thus,
234 the finding is unlikely solely due to contamination. Members of these extremophile genera are
235 known to be radiation- or ROS-resistant, which suggests a potentially plausible biological
236 mechanism for their inclusion in these communities (20). These findings suggest a possibility
237 that these ASVs might be putative indicators of patients' response to radiotherapy-based
238 treatment. . However, it is also important to note that some ASVs assigned to the same genus
239 behaved differently, such as members of the genus *Acinetobacter* (gAcine.32b4 and
240 gAcine.efe8 in Cluster A, compared to gAcine.4f58, gAcine.4c95, and gAcine.dfae in Cluster
241 C), which may reflect niche specialization within the same genus (11).

242

243 While the results suggest a clear relationship between changes in the microbiome and
244 treatment response, several open questions remain. First, previous studies in the literature
245 focused mainly on potential associations between the commensal microbiome and the
246 radiotherapy-induced side effects and comorbidities among cancer patients (12, 21-24), and
247 rarely investigated the impact of microbiome on radiotherapy efficacy except a pilot study
248 with a small sample size (n=3) which reported a relationship between the response to
249 radiotherapy and the gut microbiome in pediatric cancer patients (25). It is, however, difficult

250 to compare our findings directly with most of the published data. Replication studies will be
251 needed to determine if the microbiome can be used as a reliable indicator of treatment
252 response in NPC. In addition, we acknowledge that the majority of our study subjects were
253 NPC patients with stage III to IVb diseases (more than 90%) who were administrated
254 concurrent chemo-radiotherapy (platinum-based) as recommended by clinical guidelines, and
255 the analyses were not adjusted by therapeutic strategies due to a concern of low statistical
256 power. The response to platinum-based chemotherapy has been reported to be modulated by
257 gut microbiota, which influences the inflammation, immunity, and metabolism systematically
258 (2, 26). Our analyses could not distinguish the contributions from radiotherapy and
259 chemotherapy, separately. However, we considered that the nasopharyngeal microbiome
260 might be affected mainly and heavily by radiotherapy with high energy X-ray in the
261 nasopharynx. Last but not the least, some researchers suggest that microbiome affects the
262 response to radiotherapy by modulating the damage-associated molecular pattern signals,
263 however, the essential knowledge is yet deficient and the underlying mechanism is yet to be
264 explored (2, 4, 27). Therefore, additional work is warranted to replicate our findings among
265 similar study populations; and to address potential mechanisms, such as immune regulation
266 and potential interaction between the nasopharyngeal microbiome and systemic
267 immunotherapy.

268

269 In conclusion, this study demonstrated the temporal changes of the nasopharyngeal
270 microbiome in NPC patients during radiotherapy-based treatment and suggested a significant
271 association with clinical response. By focusing on NPC, a type of cancer where radiotherapy
272 is the most common treatment, we hypothesize that the relationship between the microbiome
273 and clinical response may hold true for other diseases and anatomical locations. These results
274 shed new light on a possibility that the commensal microbiome may influence the response to

275 radiotherapy-based anticancer treatment in cancer patients, and call for larger longitudinal
276 studies with long-term follow-up to understand the underlying mechanisms.

277

278 **Materials and Methods**

279 *Study design and setting*

280 This prospective study recruited newly diagnosed NPC patients in the First Affiliated Hospital
281 of Guangxi Medical University, Guangxi Province located in southern China, between 2014
282 and 2015. The study was approved by the Ethical Review Committee of the First Affiliated
283 Hospital of Guangxi Medical University, China, and the Regional Ethical Review Board in
284 Stockholm, Sweden. Written informed consent was obtained from all patients. A total of 76
285 NPC patients were recruited and 62 were enrolled in this study. Details are given in
286 Supplementary Data (Supplementary Method S1 and Figure S4).

287

288 All patients were treated according to the standards of clinical practice (details are given in
289 Supplementary Method S2). All patients received the first clinical check-up at 3 months after
290 the completion of radiotherapy and were followed up for 24 months. Patients who achieved a
291 complete response (CR) in the first check-up were classified as early responders and patients
292 who achieved CR between the first and the end of follow-up were designated late responders.

293

294 *Sample collection and processing*

295 In total 870 nasopharyngeal swabs were collected from 62 NPC patients. A protocol
296 including enzymatic lysis and bead beating for DNA extraction was used. The indexed library

297 targeting the V3-V4 hypervariable regions of the 16S rRNA gene was prepared using samples
298 with sufficiently high-quality DNA. Extraction controls, PCR amplification controls, and
299 bacterial reference controls were included in each step. After quality and quantity checking, a
300 total of 526 16S rRNA-based libraries and 85 control libraries were sequenced by Beijing
301 Genomics Institute (BGI, Wuhan, China), using a 300-bp paired-end strategy on Illumina
302 Miseq according to the manufacturer's instructions. Details are given in Supplementary Data
303 (Supplementary Method S3 and S4, and Figure S4).

304

305 *Data denoising and pre-processing*

306 Raw sequences were quality filtered and denoised using *deblur* to generated amplicon
307 sequence variants (ASVs) in QIIME 2 (v. 2019-10) (28-31). A phylogenetic tree was built
308 using fragment insertion into the August 2013 Greengenes 99% tree and taxonomic
309 assignments using a naïve Bayesian classifier trained against the same reference (32-34). The
310 dataset was filtered to remove samples without valid clinical information (4 individuals with
311 56 samples), ASVs assigned to mitochondrial rRNA (35), and samples with fewer than 1,500
312 reads (25 samples). Finally, 445 samples derived from 39 NPC patients were retained, with
313 around 3 million high quality reads assigned to 9,320 ASVs (33 phyla, 107 classes, 192 orders,
314 336 families, and 724 genera). Between-sample diversity (beta-diversity) was estimated after
315 samples were rarefied to 1,500 reads per sample (36). Feature-based analyses were performed
316 using a representative subset of ASVs with at least 0.1% relative abundance in at least 10% of
317 samples, as abundant ASVs (n=73). Two samples were removed due to the absence of
318 abundant ASVs, retaining 443 samples. The concordance between the main ASVs dataset and
319 the abundant ASVs subset was tested. Details are given in Supplementary Data
320 (Supplementary Method S5 and Figure S5).

321

322 *Statistical analysis*

323 In this study, the analyses of global patterns were mainly focused on beta-diversity using
324 unweighted and weighted UniFrac distance (37, 38). Principal Coordinate Analysis (PCoA)
325 projections were used to visualize between-sample difference (39). The longitudinal pattern of
326 nasopharyngeal microbiome along each principle coordinate (PC) was visualized using
327 volatility analysis in QIIME 2 2019.10 (*q2-longitudinal*) (40). The weighted UniFrac distance
328 matrix was further used to measure the rate of change which differed over treatment. The
329 change in an individual community between two sequential treatment occasions was
330 quantified as the weighted UniFrac distance between successive samples ($\Delta\text{-wUF} = \text{wUF}_{(t)} -$
331 $\text{wUF}_{(t-1)}$), corresponding to the weighted Unifrac step length of an individual's trajectory
332 through nasopharyngeal microbial space. $\Delta\text{-wUF}$ was modeled as a function of treatment
333 occasion (sampling time) via linear mixed effect models (LMEs, considering treatment,
334 temporal and inter-individual effects) with the *lme4* package (v. 1.1-19) in R 3.5.1 (41).
335 Differences between nested models were tested via likelihood ratio tests, while Akaike's
336 information criterion (AIC) was used to compare general models.

337

338 In the analyses of feature-based patterns, Non-parametric Microbial Interdependence Test
339 (NMIT) was used to determine longitudinal sample similarity as a function of temporal
340 microbial composition network over treatment (42). We further eliminated three patients who
341 had less than five successive samples, retaining 434 samples of 36 patients, to make the
342 analysis robust and efficient. In brief, the Spearman correlations between any pair of 73
343 abundant ASVs were computed based on their relative abundance; distances between any two
344 of patients' correlation matrices were calculated based on a Frobenius norm; PCoA was used

345 to visualize the similarity among patients. The difference of microbial networks between
346 response groups was tested by the permutation-based extension of multivariate analysis of
347 variance (PERMANOVA) test (43) and the multivariate dispersion test (permdisp) (44).
348 NMIT, PERMANOVA, and permdisp were carried out by QIIME 2 2019.10, and PCoA was
349 plotted in R 3.5.1. On the other hand, the longitudinal patterns of the 73 abundant ASVs
350 individually were also analyzed. The temporal relationship for the abundant ASVs was
351 evaluated using a modified analysis of composition of microbiomes (ANCOM)-based
352 approach using Spearman correlation (45). A normalized ANCOM W statistic was calculated
353 as the fraction of tests where the raw p-values were less than 0.05, and a normalized W of
354 more than 80% was considered statistically significant. This test was applied to both the raw
355 data, and the ratios between time points. Additionally, the longitudinal differences in
356 abundance (log₂-transformed) of abundant ASVs between early and late responders were
357 modeled via Smoothing-spline ANOVA (SS-ANOVA) (46) using *metagenomeSeq* package (v.
358 1.24.0); the predicted changing trajectories of abundant ASVs were grouped into hierarchical
359 clustering using Ward's method (Ward's D2) and displayed as a heatmap using *Heatplus*
360 package (v. 2.32.1) (47) in R.3.6.2.

361

362 *Data availability*

363 Raw sequencing data and metadata are deposited in ENA under accession XXXXX.

364 **Acknowledgements**

365 We acknowledge funding from the Swedish Cancer Society (2016/510 to W. Ye) and the
366 Swedish Research Council (2015-02625, 2015-06268, 2017-05814 to W. Ye); the National
367 Natural Science Foundation of China (81360405 to R. Wang) and the Guangxi (China)
368 Science and Technology Program Project (GK AD17129013 to R. Wang); the Natural
369 Science Foundation of Guangxi Medical University for Junior Scientists (GXMUYSF201203
370 to T. Huang). T. Huang was also partly supported by a grant from the China Scholarship
371 Council (201408450018).

372 We would like to thank the patients recruited in this study, and the clinical staff in the
373 Department of Radiation Oncology in the First Affiliated Hospital of Guangxi Medical
374 University (Nanning, P. R. China). We are grateful to Dr. Zhe Zhang, Dr. Xiaoying Zhou, Dr.
375 Xue Xiao, and their research group for lab support.

376 T. Huang had full access to all of the data in the study and takes responsibility for the
377 integrity of the data and the accuracy of the data analysis. T. Huang, Z. Zhang, R. Wang, and
378 W. Ye conceived and designed the study. T. Huang, R. Wang, and W. Ye received funding. T.
379 Huang, T. Zhang, and K. Hu recruited patients, collected samples and follow-up information.
380 T. Huang and X. Xiao performed laboratory assays. Z. Zhang, R. Wang, and W. Ye
381 contributed resources. T. Huang, J. Debelius, and A. Ploner analyzed the data, prepared
382 figures. T. Huang, J. Debelius, A. Ploner, R. Wang, and W. Ye interpreted the results. T.
383 Huang, J. Debelius, and A. Ploner wrote the manuscript. All authors edited the manuscript
384 and approval of the final draft.

385 On behalf of all authors, the corresponding authors declared that they have no potential
386 financial and non-financial competing interests.

387 **References**

- 388 1. Garrett WS. 2015. Cancer and the microbiota. *Science* 348:80-6.
- 389 2. Roy S, Trinchieri G. 2017. Microbiota: a key orchestrator of cancer therapy. *Nat Rev Cancer*
390 17:271-285.
- 391 3. McQuade JL, Daniel CR, Helmink BA, Wargo JA. 2019. Modulating the microbiome to improve
392 therapeutic response in cancer. *Lancet Oncol* 20:e77-e91.
- 393 4. Raza MH, Siraj S, Arshad A, Waheed U, Aldakheel F, Alduraywish S, Arshad M. 2017. ROS-
394 modulated therapeutic approaches in cancer treatment. *J Cancer Res Clin Oncol*
395 doi:10.1007/s00432-017-2464-9.
- 396 5. Geller LT, Barzily-Rokni M, Danino T, Jonas OH, Shental N, Nejman D, Gavert N, Zwang Y,
397 Cooper ZA, Shee K, Thaiss CA, Reuben A, Livny J, Avraham R, Frederick DT, Ligorio M,
398 Chatman K, Johnston SE, Mosher CM, Brandis A, Fuks G, Gurbatri C, Gopalakrishnan V, Kim M,
399 Hurd MW, Katz M, Fleming J, Maitra A, Smith DA, Skalak M, Bu J, Michaud M, Trauger SA,
400 Barshack I, Golan T, Sandbank J, Flaherty KT, Mandinova A, Garrett WS, Thayer SP, Ferrone
401 CR, Huttenhower C, Bhatia SN, Gevers D, Wargo JA, Golub TR, Straussman R. 2017. Potential
402 role of intratumor bacteria in mediating tumor resistance to the chemotherapeutic drug
403 gemcitabine. *Science* 357:1156-1160.
- 404 6. Routy B, Le Chatelier E, Derosa L, Duong CPM, Alou MT, Daillere R, Fluckiger A, Messaoudene
405 M, Rauber C, Roberti MP, Fidelle M, Flament C, Poirier-Colame V, Opolon P, Klein C, Iribarren
406 K, Mondragon L, Jacquelot N, Qu B, Ferrere G, Clemenson C, Mezquita L, Masip JR, Naltet C,
407 Brosseau S, Kaderbhai C, Richard C, Rizvi H, Levenez F, Galleron N, Quinquis B, Pons N, Ryffel
408 B, Minard-Colin V, Gonin P, Soria JC, Deutsch E, Llorca Y, Ghiringhelli F, Zalcman G,
409 Goldwasser F, Escudier B, Hellmann MD, Eggermont A, Raoult D, Albiges L, Kroemer G,
410 Zitvogel L. 2018. Gut microbiome influences efficacy of PD-1-based immunotherapy against
411 epithelial tumors. *Science* 359:91-97.

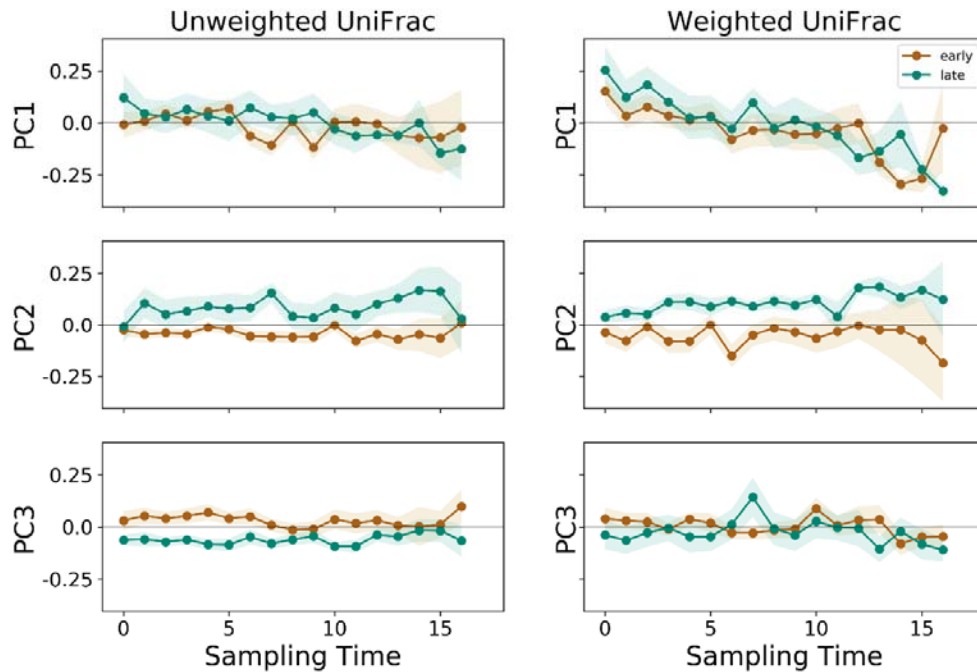
- 412 7. Helmink BA, Khan MAW, Hermann A, Gopalakrishnan V, Wargo JA. 2019. The microbiome,
413 cancer, and cancer therapy. *Nat Med* 25:377-388.
- 414 8. Chua MLK, Wee JTS, Hui EP, Chan ATC. 2016. Nasopharyngeal carcinoma. *Lancet* 387:1012-
415 1024.
- 416 9. Lee AW, Ma BB, Ng WT, Chan AT. 2015. Management of Nasopharyngeal Carcinoma: Current
417 Practice and Future Perspective. *J Clin Oncol* 33:3356-64.
- 418 10. Hong RL, Hsiao CF, Ting LL, Ko JY, Wang CW, Chang JTC, Lou PJ, Wang HM, Tsai MH, Lai SC, Liu
419 TW. 2018. Final results of a randomized phase III trial of induction chemotherapy followed by
420 concurrent chemoradiotherapy versus concurrent chemoradiotherapy alone in patients with
421 stage IVA and IVB nasopharyngeal carcinoma-Taiwan Cooperative Oncology Group (TCOG)
422 1303 Study. *Ann Oncol* 29:1972-1979.
- 423 11. Goodrich JK, Di Rienzi SC, Poole AC, Koren O, Walters WA, Caporaso JG, Knight R, Ley RE.
424 2014. Conducting a microbiome study. *Cell* 158:250-262.
- 425 12. Zhu XX, Yang XJ, Chao YL, Zheng HM, Sheng HF, Liu HY, He Y, Zhou HW. 2017. The Potential
426 Effect of Oral Microbiota in the Prediction of Mucositis During Radiotherapy for
427 Nasopharyngeal Carcinoma. *Ebiomedicine* 18:23-31.
- 428 13. Wang A, Ling Z, Yang Z, Kiela PR, Wang T, Wang C, Cao L, Geng F, Shen M, Ran X, Su Y, Cheng
429 T, Wang J. 2015. Gut microbial dysbiosis may predict diarrhea and fatigue in patients
430 undergoing pelvic cancer radiotherapy: a pilot study. *PLoS One* 10:e0126312.
- 431 14. Zaneveld JR, McMinds R, Vega Thurber R. 2017. Stress and stability: applying the Anna
432 Karenina principle to animal microbiomes. *Nat Microbiol* 2:17121.
- 433 15. Wang H, Dai W, Feng X, Zhou Q, Wang H, Yang Y, Li S, Zheng Y. 2018. Microbiota Composition
434 in Upper Respiratory Tracts of Healthy Children in Shenzhen, China, Differed with Respiratory
435 Sites and Ages. *Biomed Res Int* 2018:6515670.

- 436 16. Hang J, Zavaljevski N, Yang Y, Desai V, Ruck RC, Macareo LR, Jarman RG, Reifman J, Kuschner
437 RA, Keiser PB. 2017. Composition and variation of respiratory microbiota in healthy military
438 personnel. *PLoS One* 12:e0188461.
- 439 17. Hayes RB, Ahn J, Fan X, Peters BA, Ma Y, Yang L, Agalliu I, Burk RD, Ganly I, Purdue MP,
440 Freedman ND, Gapstur SM, Pei Z. 2018. Association of Oral Microbiome With Risk for
441 Incident Head and Neck Squamous Cell Cancer. *JAMA Oncol* 4:358-365.
- 442 18. Utter DR, Mark Welch JL, Borisy GG. 2016. Individuality, Stability, and Variability of the
443 Plaque Microbiome. *Front Microbiol* 7:564.
- 444 19. Salter SJ, Cox MJ, Turek EM, Calus ST, Cookson WO, Moffatt MF, Turner P, Parkhill J, Loman
445 NJ, Walker AW. 2014. Reagent and laboratory contamination can critically impact sequence-
446 based microbiome analyses. *BMC Biol* 12:87.
- 447 20. Battista JR, Earl AM, Park MJ. 1999. Why is *Deinococcus radiodurans* so resistant to ionizing
448 radiation? *Trends Microbiol* 7:362-5.
- 449 21. Reis Ferreira M, Andreyev HJN, Mohammed K, Truelove L, Gowan SM, Li J, Gulliford SL,
450 Marchesi JR, Dearnaley DP. 2019. Microbiota- and Radiotherapy-Induced Gastrointestinal
451 Side-Effects (MARS) Study: A Large Pilot Study of the Microbiome in Acute and Late-Radiation
452 Enteropathy. *Clin Cancer Res* 25:6487-6500.
- 453 22. Hou J, Zheng H, Li P, Liu H, Zhou H, Yang X. 2018. Distinct shifts in the oral microbiota are
454 associated with the progression and aggravation of mucositis during radiotherapy. *Radiother*
455 *Oncol* doi:10.1016/j.radonc.2018.04.023.
- 456 23. Zhang J, Liu H, Liang X, Zhang M, Wang R, Peng G, Li J. 2015. Investigation of salivary function
457 and oral microbiota of radiation caries-free people with nasopharyngeal carcinoma. *PLoS*
458 *One* 10:e0123137.
- 459 24. Wang Z, Wang Q, Wang X, Zhu L, Chen J, Zhang B, Chen Y, Yuan Z. 2019. Gut microbial
460 dysbiosis is associated with development and progression of radiation enteritis during pelvic
461 radiotherapy. *J Cell Mol Med* 23:3747-3756.

- 462 25. Sahly N, Moustafa A, Zaghoul M, Salem TZ. 2019. Effect of radiotherapy on the gut
463 microbiome in pediatric cancer patients: a pilot study. *PeerJ* 7:e7683.
- 464 26. Iida N, Dzutsev A, Stewart CA, Smith L, Bouladoux N, Weingarten RA, Molina DA, Salcedo R,
465 Back T, Cramer S, Dai RM, Kiu H, Cardone M, Naik S, Patri AK, Wang E, Marincola FM, Frank
466 KM, Belkaid Y, Trinchieri G, Goldszmid RS. 2013. Commensal bacteria control cancer response
467 to therapy by modulating the tumor microenvironment. *Science* 342:967-70.
- 468 27. Al-Qadami G, Van Sebille Y, Le H, Bowen J. 2019. Gut microbiota: implications for
469 radiotherapy response and radiotherapy-induced mucositis. *Expert Rev Gastroenterol*
470 *Hepatol* 13:485-496.
- 471 28. Bolyen E, Rideout JR, Dillon MR, Bokulich NA, Abnet CC, Al-Ghalith GA, Alexander H, Alm EJ,
472 Arumugam M, Asnicar F, Bai Y, Bisanz JE, Bittinger K, Brejnrod A, Brislawn CJ, Brown CT,
473 Callahan BJ, Caraballo-Rodriguez AM, Chase J, Cope EK, Da Silva R, Diener C, Dorrestein PC,
474 Douglas GM, Durall DM, Duvallet C, Edwardson CF, Ernst M, Estaki M, Fouquier J, Gauglitz JM,
475 Gibbons SM, Gibson DL, Gonzalez A, Gorlick K, Guo J, Hillmann B, Holmes S, Holste H,
476 Huttenhower C, Huttley GA, Janssen S, Jarmusch AK, Jiang L, Kaehler BD, Kang KB, Keefe CR,
477 Keim P, Kelley ST, Knights D, et al. 2019. Reproducible, interactive, scalable and extensible
478 microbiome data science using QIIME 2. *Nat Biotechnol* 37:852-857.
- 479 29. Bokulich NA, Kaehler BD, Rideout JR, Dillon M, Bolyen E, Knight R, Huttley GA, Gregory
480 Caporaso J. 2018. Optimizing taxonomic classification of marker-gene amplicon sequences
481 with QIIME 2's q2-feature-classifier plugin. *Microbiome* 6:90.
- 482 30. Amir A, McDonald D, Navas-Molina JA, Kopylova E, Morton JT, Zech Xu Z, Kightley EP,
483 Thompson LR, Hyde ER, Gonzalez A, Knight R. 2017. Deblur Rapidly Resolves Single-
484 Nucleotide Community Sequence Patterns. *mSystems* 2.
- 485 31. Bokulich NA, Subramanian S, Faith JJ, Gevers D, Gordon JJ, Knight R, Mills DA, Caporaso JG.
486 2013. Quality-filtering vastly improves diversity estimates from Illumina amplicon sequencing.
487 *Nat Methods* 10:57-9.

- 488 32. McDonald D, Price MN, Goodrich J, Nawrocki EP, DeSantis TZ, Probst A, Andersen GL, Knight
489 R, Hugenholtz P. 2012. An improved Greengenes taxonomy with explicit ranks for ecological
490 and evolutionary analyses of bacteria and archaea. *ISME J* 6:610-8.
- 491 33. Wang Q, Garrity GM, Tiedje JM, Cole JR. 2007. Naive Bayesian classifier for rapid assignment
492 of rRNA sequences into the new bacterial taxonomy. *Appl Environ Microbiol* 73:5261-7.
- 493 34. Janssen S, McDonald D, Gonzalez A, Navas-Molina JA, Jiang L, Xu ZZ, Winker K, Kado DM,
494 Orwoll E, Manary M, Mirarab S, Knight R. 2018. Phylogenetic Placement of Exact Amplicon
495 Sequences Improves Associations with Clinical Information. *mSystems* 3.
- 496 35. Emelyanov VV. 2001. Evolutionary relationship of Rickettsiae and mitochondria. *FEBS Lett*
497 501:11-8.
- 498 36. Weiss S, Xu ZZ, Peddada S, Amir A, Bittinger K, Gonzalez A, Lozupone C, Zaneveld JR,
499 Vazquez-Baeza Y, Birmingham A, Hyde ER, Knight R. 2017. Normalization and microbial
500 differential abundance strategies depend upon data characteristics. *Microbiome* 5:27.
- 501 37. Lozupone CA, Hamady M, Kelley ST, Knight R. 2007. Quantitative and qualitative beta
502 diversity measures lead to different insights into factors that structure microbial
503 communities. *Appl Environ Microbiol* 73:1576-85.
- 504 38. Lozupone C, Knight R. 2005. UniFrac: a new phylogenetic method for comparing microbial
505 communities. *Appl Environ Microbiol* 71:8228-35.
- 506 39. Vazquez-Baeza Y, Pirrung M, Gonzalez A, Knight R. 2013. EMPeror: a tool for visualizing high-
507 throughput microbial community data. *Gigascience* 2:16.
- 508 40. Bokulich NA, Dillon MR, Zhang Y, Rideout JR, Bolyen E, Li H, Albert PS, Caporaso JG. 2018. q2-
509 longitudinal: Longitudinal and Paired-Sample Analyses of Microbiome Data. *mSystems* 3.
- 510 41. Bates D, Mächler M, Bolker B, Walker S. 2015. Fitting Linear Mixed-Effects Models Using
511 lme4. 2015 67:48.

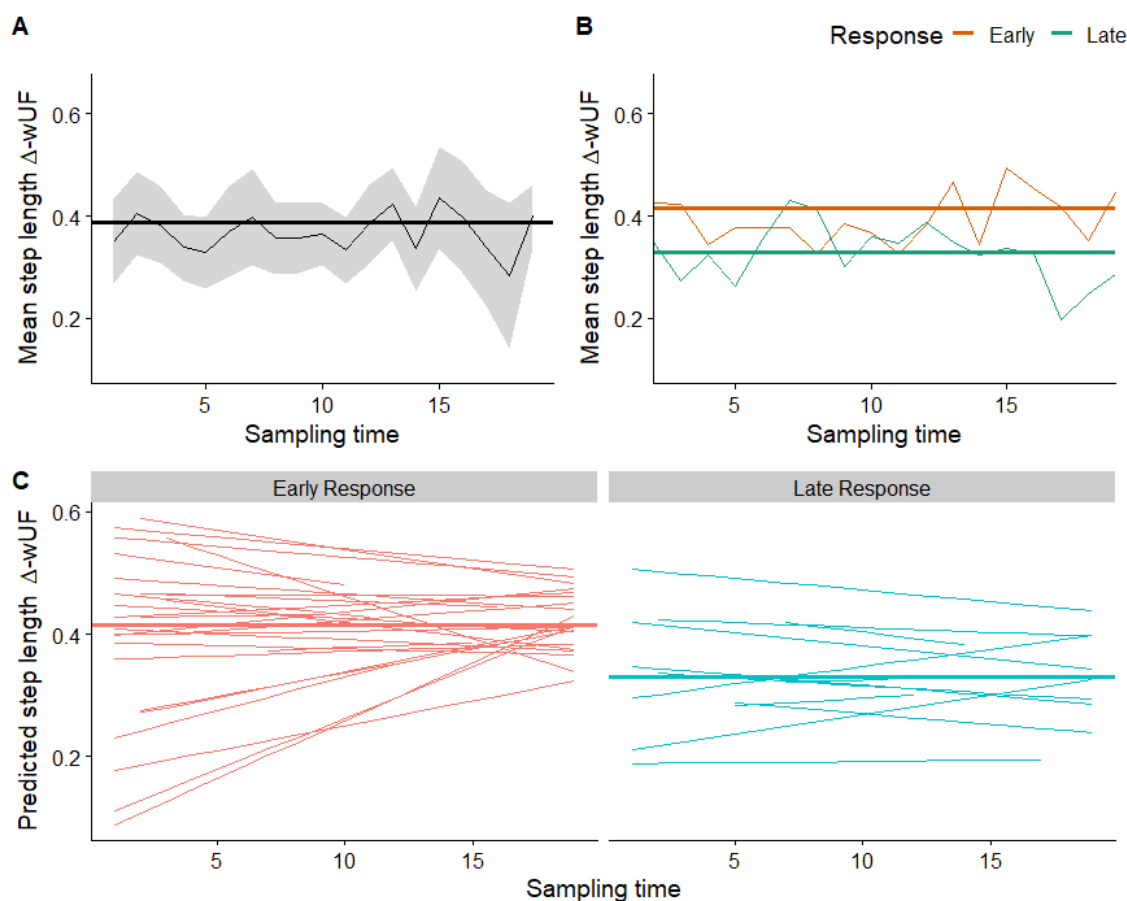
- 512 42. Zhang Y, Han SW, Cox LM, Li H. 2017. A multivariate distance-based analytic framework for
513 microbial interdependence association test in longitudinal study. *Genet Epidemiol* 41:769-
514 778.
- 515 43. Anonymous. *Permutational Multivariate Analysis of Variance (PERMANOVA)*, p 1-15, Wiley
516 StatsRef: Statistics Reference Online doi:10.1002/9781118445112.stat07841.
- 517 44. Anderson MJ, Ellingsen KE, McArdle BH. 2006. Multivariate dispersion as a measure of beta
518 diversity. *Ecol Lett* 9:683-93.
- 519 45. Mandal S, Van Treuren W, White RA, Eggesbo M, Knight R, Peddada SD. 2015. Analysis of
520 composition of microbiomes: a novel method for studying microbial composition. *Microb*
521 *Ecol Health Dis* 26:27663.
- 522 46. Joseph N. Paulson HT, Hector Corrada Bravo. 2017. Longitudinal differential abundance
523 analysis of microbial marker-gene surveys using smoothing splines. *bioRxiv*
524 doi:<https://doi.org/10.1101/099457>.
- 525 47. Ploner A. 2018. Heatplus: Heatmaps with row and/or column covariates and colored clusters.
526 <https://github.com/alexploner/Heatplus>,
- 527



528

529 **Figure 1. Normalized volatility of the nasopharyngeal microbiome in 39 patients during**
530 **a 7-week treatment course.**

531 The longitudinal pattern of the nasopharyngeal microbiome of 39 patients over 7-week
532 treatment was explored by Principle Coordinate Analysis (PCoA) projection along principle
533 coordinate1 (PC1), PC2 and PC3 with regard to sampling time. The volatility analysis was
534 used to visualize the mean distances based on UniFrac distance matrices in each PC space.
535 The left of each panel reflects mean volatility of all individual trajectories referred to the
536 unweighted UniFrac distance matrix, and the right side referred to the weighted UniFrac
537 distance matrix. The consecutive numbers on the bottom indicate the sampling time points (0
538 = before radiotherapy). The trace represents the mean and the shaded is the standard deviation
539 of each sampling time point. The curves in each PC space are marked by response status (a
540 brown curve showing the early responders, a green curve showing the late responders).

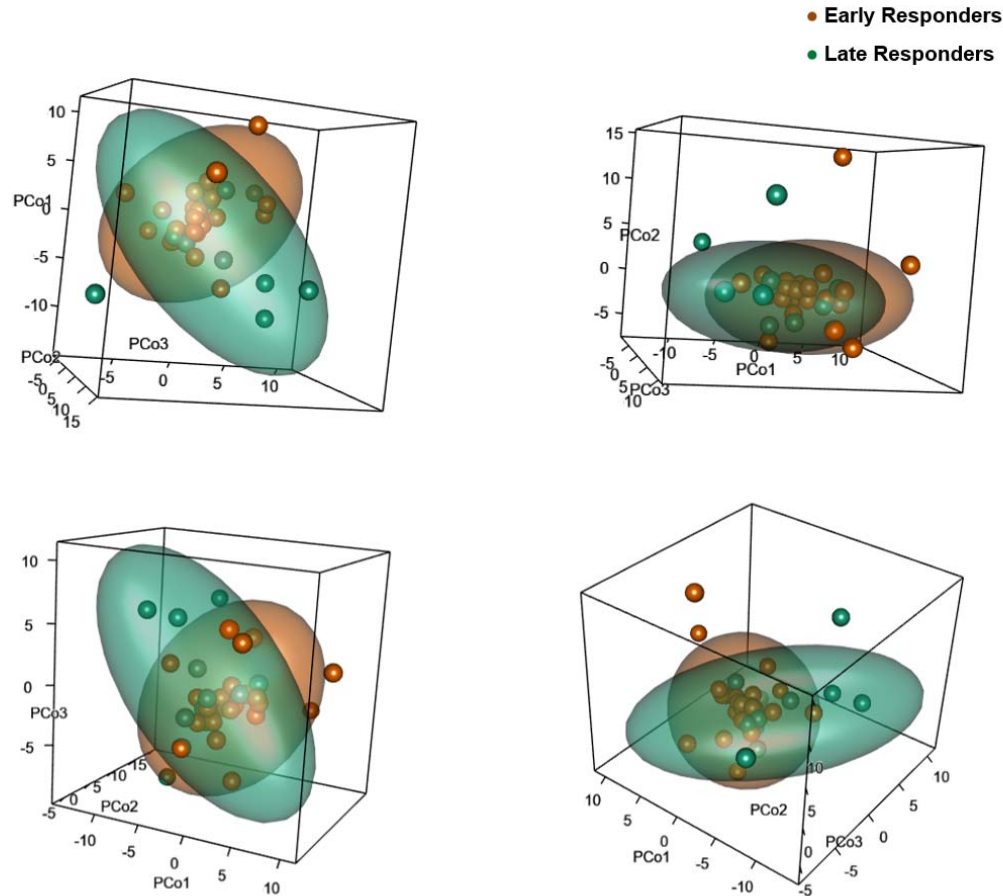


541

542 **Figure 2. Group-wise and individual Δ -wUFs during treatment reflect the rate of change**
543 **in the community.**

544 The weighted UniFrac step length Δ -wUF of an individual's trajectory through
545 nasopharyngeal microbial space was modeled as a function of treatment occasion (sampling
546 time) via linear mixed effect models (LMEs), including within-individual random effects. The
547 consecutive numbers on the bottom of each panel indicate the sampling time points. We
548 explored (Panel A) the average step length across all individuals and (Panel B) average step
549 length by clinical response. The moving average is shown as a thin line with shaded pointwise
550 95% confidence intervals; the thicker line is the estimated average step length (fixed effect)
551 from the mixed model which takes into account the individual-level variations in step length
552 over sampling time. We also explored the predicted individual step length trajectories for

553 early and late responders (Panel C). The horizontal axis indicates the sampling time during
554 treatment and the vertical axis the mean step length Δ -wUFs.



555

556 **Figure 3. Differences in the interdependence networks of nasopharyngeal microbiome**
557 **between the early and late responders.**

558 Non-parametric microbial interdependence test (NMIT) was used to determine longitudinal
559 sample similarity as a function of temporal microbial composition networks over treatment.

560 The similarities of nasopharyngeal microbial networks among NPC patients were visualized

561 by Principle Coordinate Analysis (PCoA) projection. The first 3 axes in PCoA explain 15.03%

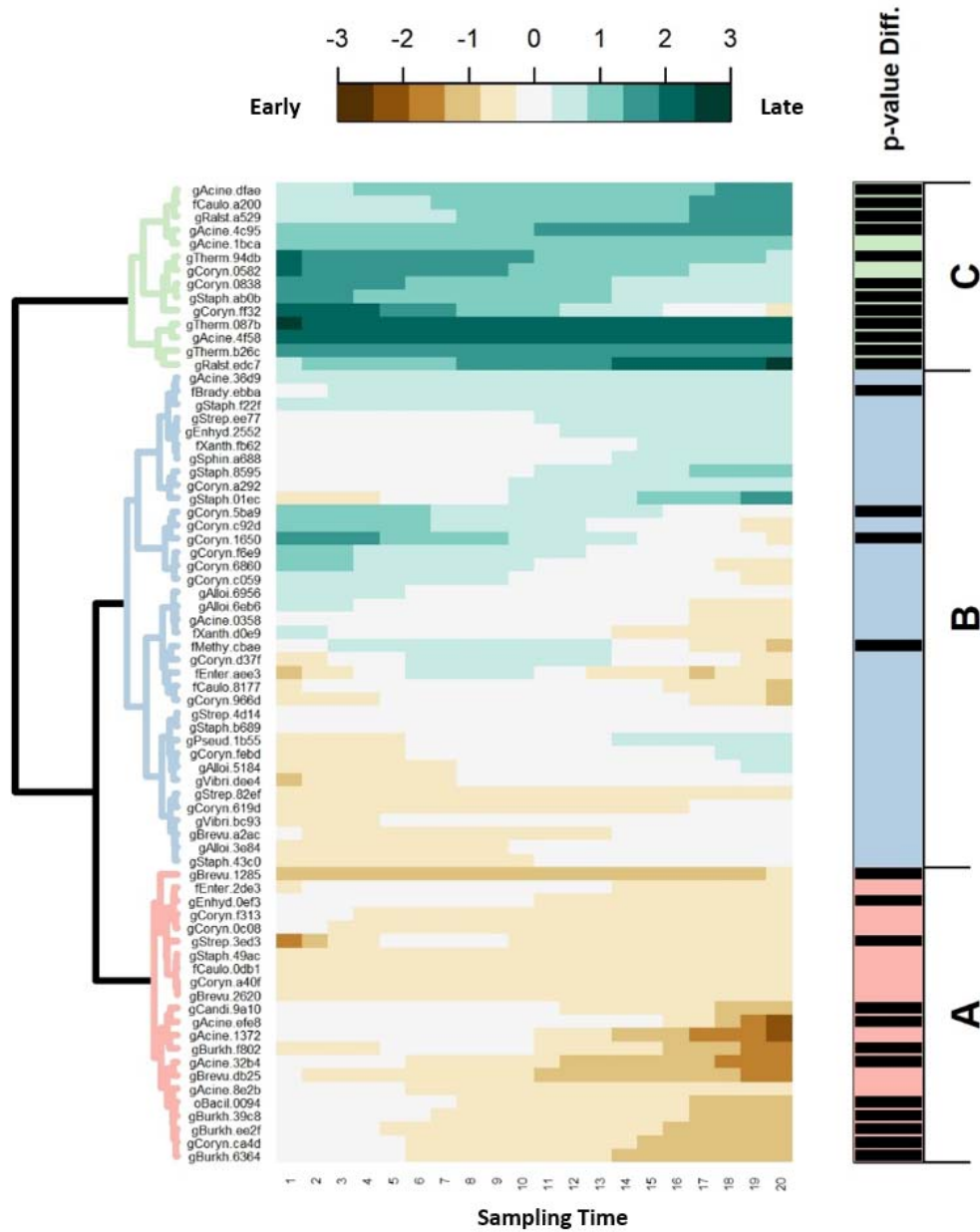
562 of the variation in total (PCo1=5.67%, PCo2=4.91%, PCo3=4.45%). Each dot in the PCoA

563 space is an indicator representing the temporal microbial network of one NPC patient. Brown

564 dots are the early responders, green the late responders. The cloud representing the minimum-

565 volume ellipsoid covers 80% of the data of each group. Panels A-D reflect different

566 orientations of the same 3-dimension plot (screenshots from a 3-dimension PCoA projection).



567

568 **Figure 4. The predicted log₂-fold change trajectories of 73 abundant ASVs between the**
569 **early and late responders.**

570 The predicted log₂-fold change trajectories of 73 amplicon sequence variants (ASVs) between
571 the early responders and late responders generated from SS-ANOVA were grouped into
572 hierarchical clusters using Ward's D2 and displayed as a heatmap. Each row in the heatmap
573 represents the trajectory across treatment of each ASV. The consecutive numbers on the
574 bottom of heatmap indicate the sampling time points (1 = before radiotherapy, 20 = end of
575 radiotherapy). ASVs with higher abundance in early responders are brown; those with more
576 abundance in late responders are teal. Three clusters are marked as A to C. The vertical bars
577 on the right side indicate whether the trend in difference across treatment is statistically
578 significant (P -value < 0.05 for the black bars, otherwise not).

579 **Table 1. Twenty-eight abundant ASVs were detected with significant differences**
 580 **between early and late responders during a 7-week treatment course.**

ASV-ID	Taxonomy ^a	Time intervals ^b		Permutative ^c
		Start	End	P-value
gBurkh.6364	g__Burkholderia	7	20	0.005
gBurkh.39c8	g__Burkholderia	8	20	0.007
gCandi.9a10	g__Candidatus Rhodoluna	14	20	0.009
oBacil.0094	o__Bacillales	8	20	0.011
gAcine.32b4	g__Acinetobacter	7	20	0.011
gAcine.efe8	g__Acinetobacter	18	20	0.011
gEnhyd.0ef3	g__Enhydrobacter	10	20	0.018
gStrep.3ed3	g__Streptococcus	1	17	0.020
gBrevu.1285	g__Brevundimonas	1	19	0.024
gCoryn.ca4d	g__Corynebacterium	8	20	0.029
gBurkh.f802	g__Burkholderia	14	20	0.044
gBurkh.ee2f	g__Burkholderia	7	20	0.049
fMethy.cbae	f__Methylobacteriaceae	5	11	0.017
gCoryn.1650	g__Corynebacterium	1	12	0.026
fBrady.ebba	f__Bradyrhizobiaceae	6	20	0.029
gCoryn.5ba9	g__Corynebacterium	1	13	0.043
gTherm.b26c	g__Thermus	1	20	0.003
fCaulo.a200	f__Caulobacteraceae	2	20	0.003
gTherm.94db	g__Thermus	1	19	0.003
gTherm.087b	g__Thermus	1	20	0.004
gAcine.4f58	g__Acinetobacter	1	20	0.005
gRalst.edc7	g__Ralstonia	1	20	0.006
gAcine.4c95	g__Acinetobacter	1	20	0.009
gAcine.dfae	g__Acinetobacter	1	20	0.013
gCoryn.ff32	g__Corynebacterium	1	12	0.016
gStaph.ab0b	g__Staphylococcus	1	14	0.021
gCoryn.0838	g__Corynebacterium	1	15	0.025
gRalst.a529	g__Ralstonia	4	20	0.041

581 ^a: Taxonomy assignment. “g__” refers to genus; “f__” refers to family; “o__” refers to order.

582 ^b: Time intervals with significant difference; number refers to sampling time (1 = before radiotherapy,

583 20 = end of radiotherapy).

584 ^c: 1500 permutations.